RESEARCH ON THE PROCESSES, CHARACTERIZATION AND APPLICATION AREAS OF Cu-Zr-Al-Ag BASED VARIOUS FORMS AMORPHOUS ALLOYS

PhD Thesis – Abstract

for obtaining the scientific title of doctor from
Politehnica University Timisoara
in the PhD field of MATERIALS ENGINEERING

author ing. Hididis Petru
scientific coordinator Prof.univ.dr.ing. Viorel Aurel ȘERBAN

month 11 year 2024

Introduction

The starting point of this PhD thesis is the study of metallic alloys with amorphous structure, known as metallic glasses when produced by cooling from a melt. Unlike traditional crystalline materials, amorphous alloys have a partially chaotic atomic arrangement, giving them, depending on their composition, a unique set of properties such as high mechanical strength, high hardness, enhanced corrosion resistance, and exceptional magnetic and electrical properties. Research into these materials is continuously advancing [1] and as technology progresses, their applications have begun to expand [2]. Amorphous alloys based on Cu-Zr and Cu-Zr-Al have attracted significant attention in recent years due to their remarkable combination of mechanical, chemical, and thermal properties [3-5]. One of the most notable attributes of these alloys is their high elastic limit, allowing them to withstand substantial deformation without permanent damage—a key feature for applications requiring high durability and strength. Additionally, their amorphous nature provides superior corrosion resistance, a critical property for biomedical devices and components, making them suitable for use in corrosive industrial environments. They also exhibit excellent glass-forming ability, meaning they can be processed into complex shapes with ease—a significant advantage for manufacturing components with intricate geometries.

Chapter 1 Aim of thesis

Context

In cutting-edge technologies, high-purity elements are used to produce metallic alloys with an amorphous structure [6, 7]. The reliability of such structures is also ensured by the controlled atmosphere in which they are produced: argon and vacuum, to prevent contamination during the process. Thus, obtaining amorphous metal alloys requires extremely precise preparation conditions.

A major motivation for this thesis regarding the production of Cu-Zr-based amorphous alloys is the high production cost associated with the manufacturing process. The production conditions, essential for obtaining these special high-quality alloys, significantly increase the overall production cost. Consequently, their use occurs in a limited number of industries.

The thesis focuses on the production of amorphous alloys with the main chemical elements Cu-Zr, using elements with medium technical purity (usually with purity levels between 99.0% and 99.9%) and current processing methods designed for this purpose. By

additionally introducing new chemical elements, such as Al and Ag, the aim is to enhance the ability to achieve amorphization and to maintain the desired properties of these alloys, such as high strength and corrosion resistance. Reducing dependence on high-purity elements could have a substantial economic impact by lowering material costs. Consequently, the production process becomes more accessible for large-scale industrial applications. Utilizing a facility with a simplified argon protection system, which is easier to maintain while still providing a sufficiently inert environment for many metallurgical processes, streamlines the production process while ensuring the quality of the resulting amorphous alloys.

The alloying of ternary Cu-Zr alloys with Al and Ag improves mechanical and thermal properties while also helping to prevent defects that may arise in the material. Additionally, alloying with Ag enhances the alloy's plastic range due to improved ductility[8]. Furthermore, silver improves the stability of the alloy during cooling, increasing the capacity for amorphization and certain thermal properties [9-11]. Another attribute of Ag is that it enhances electrical and thermal conductivity, making the alloy more suitable for applications that require both mechanical strength and efficient energy transfer.

Motivation

Therefore, the goal of this thesis is to obtain Cu50-xZr45Al5Agx based amorphous alloys from common medium technical purity elements, with specific properties, that allow their use in various applications.

The main objectives are:

- Production of Cu-Zr and Cu-Zr-Al based alloys with an amorphous structure by alloying with Ag under ribbon and rod shape
- Characterization of the obtained alloys from regarding their structural, mechanical, and chemical properties
- Developing applications in the field of manufacturing composites and devices such as porous nanostructures

Consequently, the experimental program is focused on research aimed both at obtaining Cu-Zr-Al metallic glasses, additionally alloyed with Ag, from chemical elements with medium technical purity, but also their mechano-chemical properties investigations, as well as their integration into applications such as composites or even nanoporous structures using the technologies identified and developed within the thesis.

Chapter 2 State of the art

Materials with an amorphous structure provide a distinctive understanding of how a non-equilibrium liquid structure forms a final product in various structural states. By abruptly halting the crystallization process during cooling, the structural state of the liquid phase is preserved (frozen), resulting in the amorphous state. For this reason, metallic amorphous alloys obtained by "freezing" the molten structure (liquid phase) are also referred to as metallic glasses. The interest in producing these metallic glasses in the form of large-sized "products" has seen impressive development in recent decades due to their expanding applicability. Their mechanical properties are the main factor promoting them as unique materials. Low Young's modulus, good yield strength, significant elastic strain limit, and corrosion resistance are factors that have heightened interest in applying these products in various fields.

The chemical composition can be calibrated according to the purpose and applicability of the final product. Biomedical products must be biocompatible with the human body, aerospace components need to withstand extreme temperature and pressure changes, and

automotive products are subjected to a wide range of vibrations. To verify the success of each product, mechanical, thermodynamic, and corrosion tests are conducted. To prevent damage, certain alloying elements are added to the nominal chemical composition. Technical studies aimed at creating joints between amorphous alloys with a thickness of no more than 60 μm are continuously evolving. The welding joining method allows for the creation of products in various and complex shapes, thereby further increasing their applicability in industry.

Through the dealloying process, nanoporous structures containing networks within the material are created, which offer new and distinct properties to the alloys. Dealloying is a selective process in which the elements in the material's composition are dissolved. Copper-based alloys are known for their favorable dealloying behavior, as they create nanoporous structures due to the presence of intermetallic compounds and modified morphology that allow for a uniform distribution of nanopores [12]. This promising process has paved the way for applications in creating superhydrophobic surfaces applicable to water and oil separation [13].

Glass forming ability

The glass forming ability (GFA) indicates a melt's tendency to vitrify and expresses its capacity to suppress crystal nucleation. Determining this parameter offers a simpler and quicker way to identify and design new alloy compositions that are prone to forming amorphous structures. The first Cu-Zr-based alloys with high glass forming ability were identified in the Cu-Zr-Ti [14] and Cu-Zr-Al [15] alloy systems. Since viscosity and relaxation time are interconnected and time-dependent, a high rapid relaxation time of a melt can exceed equilibrium, lacking sufficient time to adapt to new conditions. When a high cooling rate is applied (approximately 10^4-10^6 K/s for metallic glasses), atoms do not have enough time to form a crystalline network, leading to an imbalance in the liquid state [16].

The ability of a melt to become amorphous is assessed by the critical cooling rate. This rate represents the minimum cooling speed required to maintain the melt in an amorphous state to avoid crystallization, and it is quite challenging to determine. Parameters have been proposed for evaluating the capacity for amorphization that have become widely used:

- Reduced glass transition temperature: $T_{rg}=T_g/T_l$
- Supercooled liquid region: $\Delta T_{xg}=T_x-T_g$
- Parameter $\gamma=T_x/(T_g+T_l)$

(where T_g is the glass transition temperature, T_x is the crystallization temperature, and T_l represents the liquidus temperature)

Under certain conditions, when a supercooled liquid in the transition region is subjected to temperature variations, a time-dependent change in volume and enthalpy occurs, along with atomic rearrangement. This process is known as structural relaxation.

The relaxation time has a significant influence on the glass formation process, as it is temperature-dependent; if not carefully correlated, devitrification can occur due to the development of pre-existing nuclei. Issues arising in the realm of amorphous alloys are attributed to the temperature dependence of the mean relaxation time and are related to the medium-range order of the spatial arrangement of atoms [17].

The Angell plot, illustrated in figure 1, is a method for comparing the temperature dependence of viscosity for different alloys capable of forming an amorphous structure. The logarithm of viscosity is plotted against T_g/T. The graph shows a range of behavior, from "strong" to "fragile," for various metallic alloys, as well as organic and silicate alloys

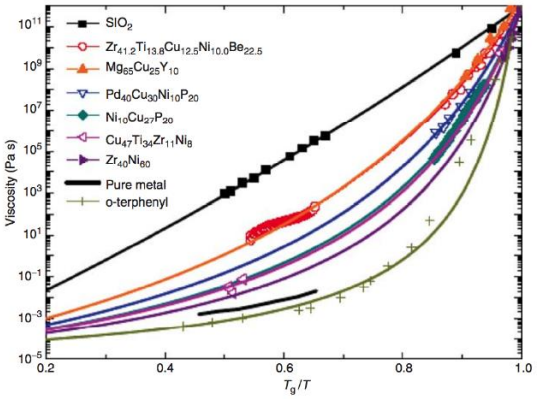

Fig. 1: Angell plot

Elastic properties should be viewed as a parameter of brittleness. A high density maintains the bonding configuration and thus prevents the redistribution of atoms, resulting in a low Poisson's ratio and a strong tendency for the alloy to vitrify. Figure 2 shows the correlation between the critical rate and the Poisson's ratio for oxide glasses, bulk metallic glasses (BMG), and conventional metallic glasse [18].

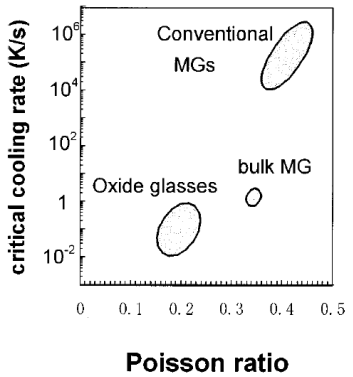

Fig. 2: Relation of cooling rate and Poisson's ratio

Amorphous alloys categories

Amorphous alloys can be classified into different categories based on their elemental composition and the mechanisms that lead to the formation of their disordered structures. A common classification, as described by H. S. Chen in his work on metallic glasses, divides binary amorphous alloys into the following categories [19]:

- Nobel metal alloys, with 10-30%: P, B, Si, C
- Transition metal: Zr, Nb, Ta, Ti, Fe, Co, Ni, Cu, Pd
- Group IIA metals: Mg, Ca, Be

Tabel 1 Categories and systems of alloys:

Category	System	Composition interval of x
Nobel metal alloys	$Au_{100-x}Si_x$	18.6-30
	$Pd_{100-x}Si_x$	15-23
	$Ni_{100-x}P_x$	8.6-26.2
	$Fe_{80}B_{20}$	
Transition metal	$Zr_{100-x}Ni_x$	20-40
	$Zr_{100-x}Cu_x$	40-75

	$Zr_{72}Co_{28}$
	$Nb_{60}Rh_{40}$
Group IIA metals	$Mg_{60}Sb_{40}$
	$Mg_{65}Cu_{35}$

Cu-Zr based alloys

Equilibrium Cu-Zr alloys exhibit remarkable differences compared to amorphous structures due to their ability to form well-defined intermetallic compounds with distinct atomic arrangements.

A series of intermetallic phases can lead to the formation of crystalline phases within the Cu-Zr alloy. With their regular and ordered atomic structure, these phases are stable at specific compositions and temperatures. For the Cu-Zr system, the crystalline phases of significance are:

- B2 CuZr
- $CuZr_2$
- $Cu_{10}Zr_7$

Observing this limitation of specific composition for bulk metallic glasses, Cu-Zr alloys can be alloyed with various elements. This alloying can help improve certain characteristics such as strength, ductility, and thermal stability. The main advantage of the ternary Cu-Zr-Al alloys is their ability to enhance the glass-forming ability, due to the supercooled liquid region and the position of the T_g relative to the T_l. With the addition of Al, the crystalline phases should circumvent the formation of intermetallic phases, due to the formation of Al-Cu and Al-Zr bonds. These bonds have also been shown to improve the glass-forming ability [20].

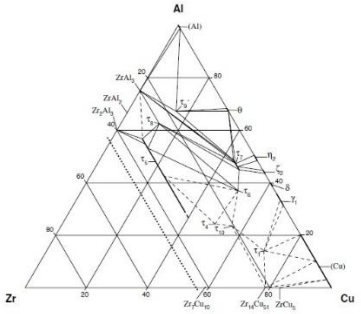

Fig. 3: Cu-Zr-Al system at 500°C

Referring to the ternary diagram (Fig. 3), Wang et al. established that the alloy with the highest glass-forming ability is $Cu_{58.1}Zr_{35.9}Al_6$. The "cluster" lines criteria was used to determine a specific composition from the ternary diagram: the third element of the composition is related to a binary group composition. The argument is that with the addition of Al, the T_x has increased, leading to a more stable and improved Cu-Zr group, and also increasing T_g, which results in a higher viscosity that contributes to reducing the cooling rate of the crystalline phases.

Fundaments and aspects of the methods of fabrication

In order to obtain amorphous alloys, the fast solidification of the melt must respect two principles:

- The solidification process must assure a cooling speed greater than the critical speed that avoids crystallization
- The solidification process must allow to cool the alloy until a temperature below the recrystallization temperature of the alloy is reached

To obtain amorphous solids using fast cooling of the melt, cooling speeds higher than 10^4-10^5 K/s are needed. These speeds are obtained if a value high enough for the thermal coefficient at the meld-cooling medium interface is assured and if the thickness of the solid is small enough so that the heat can be eliminated in a very short span of time (in order to avoid crystallization).

To produce amorphous alloys on a large scale, it is necessary to use continuous procedures of cooling of a melt. These techniques have the advantage of obtaining products by direct casting and not by processing the semi-finished products. One of the most used techniques that offers large quantities of end products is the melt spinning technique. It is widely used in laboratories and production units, becoming "a standard" for producing amorphous alloys [21].

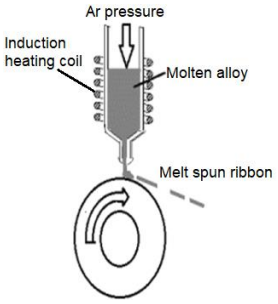

Fig. 4: Melt spinning

The primary alloy (master alloy), with a chemical composition conducive to amorphization and obtained in advance through conventional casting, is melted in a crucible and forced through the crucible's discharge slot by applying pressure, coming into contact with the surface of the cooling roll rotating at a speed that ensures the continuous formation of ribbons with an amorphous structure. It is essential to maintain a constant speed of the molten alloy jet.

Applications of metallic glass alloys

There are numerous applications for these alloys due to their specific properties. One common example is a sensor used as a biomedical device for measuring various physiological functions (such as monitoring joint movements). It consists of an amorphous metal ribbon with micrometer thickness (around 30 μm) that exhibits high magnetostriction.

In the case of the alloys studied in this thesis, particularly those based on Cu-Zr, they have been utilized in the form of ribbons to create pressure sensors for the automotive industry (see Fig. 5). Their advantages include small size, high sensitivity, and much greater pressure resistance, which cannot be achieved with stainless steel diaphragms.

Fig. 5: Zr-based BMG diaphragms

The automotive industry made use of amorphous alloys by implementing them in products that make use of spring features. Valve springs implements such products, and by using amorphous alloys it is possible to decrease the weight of the engine and consequently reducing the fuel consumption.

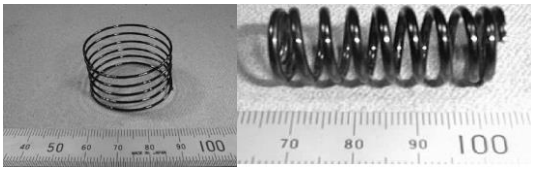

Fig. 6: Valve springs

Amorphous alloys have proven advantageous in sports equipment, such as golf clubs and tennis rackets. Golf clubs made from bulk metallic glasses exhibit superior performance due to their ability to maximize the coefficient of restitution upon impact between the club and the ball. Compared to titanium-based golf club heads, those with amorphous alloy heads displayed a significantly higher coefficient, extending the ball's flight distance by approximately 13 meters.

The aerospace industry has implemented amorphous alloys to cover leading-edge flaps (the elements that modify lift force). Traditionally, these parts are produced through complex manufacturing processes. The higher strength and hardness of metallic glass-based systems can be beneficial for these aerospace applications.

Chapter 3 Methodology and experimental procedures

Equipment used for investigations

In this chapter, the equipment used for investigations in this thesis is presented.

To produce the materials, it was used:

- Arc remelter and suction casting for micro and nanofabrication (AM 500)
- Cutting machine (Minitom, Struers)
- Equipment for amorphous alloy elaborating by melt spinning
- Ultrasonic welding equipment
- Spot welding

For investigations:

- X-ray diffractometer (X'Pert³ Powder, Philips)
- Confocal Laser scanning microscope (VK-X260K, Keyence)
- Scanning electron microscope (FEI Inspect-S)
- Micro Vickers hardness tester (ZHVμ-M, ZwickRoell)
- Differential scanning calorimetry (STA 449F1, Netzsch)
- Nanoindentation tester (NHT3, Anton Paar)

- Spectrophotometer UV-Vis-NIR Lambda 950

In order to process the results, the software that were used are:

- STA 449 F1 Netzsch Data collector
- X' pert data collector, XRD Philips
- X' pert highscore plus, PANalystical
- TestXpert ZHVμ
- Microsoft office package
- Anton Paar AP Connect

Sample preparation master alloys

The production of metallic alloys in the form of ribbons and rods involves two main stages.

The first stage consists of the development of master alloy. Based on the analyses conducted, it has been determined that experimental studies will focus on Cu-Zr-Al-based alloys with additional Ag additions. The targeted chemical compositions are $Cu_{50-x}Zr_{45}Al_5Ag_x$, where x = 0, 5, or 10. The raw materials used are of medium technical purity in the form of wires (Cu, Al), powder (Zr), and bars of Ag (granules).

For a batch of master alloy, the necessary quantities of chemical elements are specified in Table 2.

Tabel 2 Components weights for the studied chemical compositions

Chemical composition	Cu (g)	Zr (g)	Al (g)	Ag (g)
$Cu_{50}Zr_{45}Al_5$	4.28	5.53	0.18	-
$Cu_{45}Zr_{45}Al_5Ag_5$	3.74	5.37	0.18	0.71
$Cu_{40}Zr_{45}Al_5Ag_{10}$	3.23	5.22	0.17	1.37

After weighing and mixing them in a crucible, the alloy was processed and cast into cylindrical discs, known as "buttons" (figure 7) using a vacuum arc melting setup. After cooling, the master alloys were extracted and weighed. Regarding mass, the efficiency of this method ranged from 92.45% to 100%

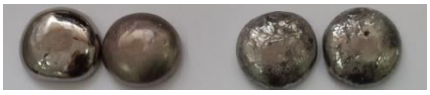

Fig 7: Master alloy

Sample preparation metallic glasses ribbons

The actual production of the amorphous structure ribbons represented the second stage of the process. The ribbons were obtained using the equipment for producing amorphous metals-melt spinning developed within the Department of Materials Engineering and Fabrication. The main parameters used to produce the ribbons are presented in Table 3.

Tabel 3 Melt spinning parameters

Parameter	Value	Units
Argon Pressure	500-600	mbar
Copper Wheel Rotation Speed	2000	rpm
Crucible-Wheel Distance	0.4-1	mm
Distance tip of crucible-copper wheel	0.4	mm
Mass of master alloys	20	g

Fig. 8: Amorphous ribbons

Sample preparation of rods

The master alloys, melted by induction, were ejected into a mold made of copper or an alloy of copper (which had the option of being cooled). The mold is composed of two symmetrical halves, secured with four screws. Rods with diameters ranging between 1 and 3 mm were obtained (figure 9).


Fig. 9: Rod obtained in a Cu mold

Chapter 4 Methods of investigation and characterization

This chapter presents the investigations conducted to characterize the obtained alloys. Their structure was analyzed using XRD, morphology was examined with an electron microscope, and thermal properties were assessed using differential scanning calorimetry. Mechanical properties were determined using a microhardness tester, nanoindentation equipment, and a tensile testing machine. Chemical properties were evaluated by measuring the conductivity of a quantity of deionized water in which samples were immersed for various periods at elevated temperatures.

Characterization of master alloys, ribbons and rods

For the master alloys, the crystalline structure was confirmed using X-ray diffraction, and the scanning electron microscope revealed the absence of pores, indicating that the vacuum arc remelting method successfully produces master alloys.

The amorphous structure of the ribbons was confirmed through XRD. In the case of the composition without Ag, crystalline phase peaks were observed on the diffractograms.

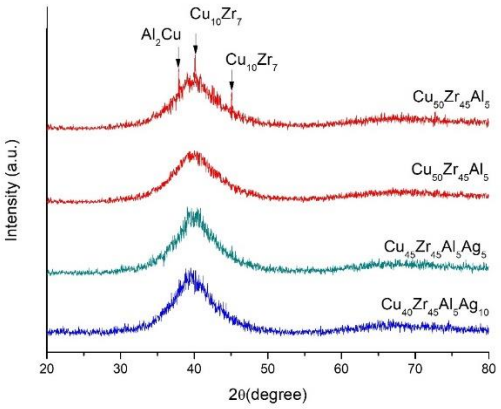

Fig. 10: XRD analysis on ribbons

Using DSC, the parameters T_{rg}, ΔT_{xg} și γ were calculated using the formulas previously mentioned. These parameters indicated that the ribbons containing Ag have higher values for γ, which suggests a better GFA compared to those without Ag.

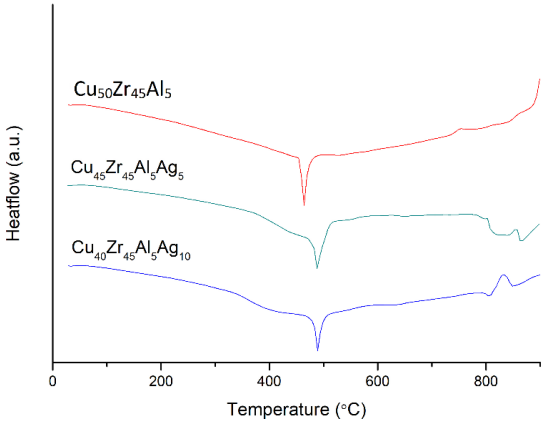

Fig. 11: DSC results on ribbons

For the rods, the amorphous structure was only observed in the case of the highest Ag concentration. Similarly, the XRD did not suggest a glass transition temperature for the other compositions.

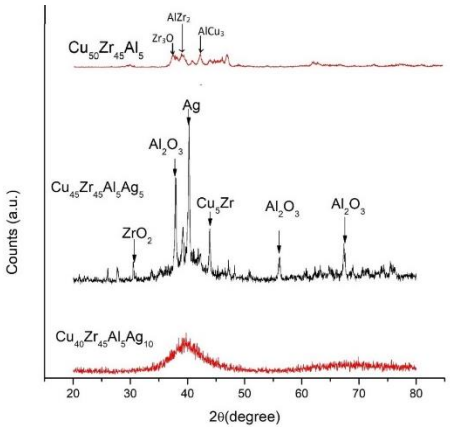

Fig. 12: XRD on rods

By using the vacuum arc re-melting method, master alloys were successfully obtained. The amorphous structure of the ribbons was confirmed using XRD, and DSC along with the calculation of parameters for evaluating the glass-forming ability indicated superior capacity in the ribbons containing Ag. The ribbons with the composition $Cu_{50}Zr_{45}Al_5$ showed low T_x values, suggesting lower thermal stability. To achieve an amorphous structure in the rods, it is necessary to either increase the silver concentration or enhance the cooling rate.

Characterization of mechanical properties: Hardness and Nanoindentation

This subsection aims to evaluate the hardness characteristics of the samples. The hardness determination was performed using micro-Vickers hardness tests on the Shimadzu HMV 2T equipment, in accordance with DIN EN ISO 6507 and ASTM E384 standards. The nanoindenter used for investigating the samples in this study was provided by the Department of Materials Engineering and Fabrication and was an Anton Paar Step 500 equipped with an NHT³ nanoindentation tester. The latter was applied exclusively to the ribbons.

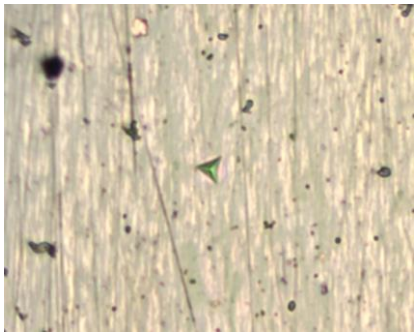

Fig. 13: Berkovich indentation

Higher hardness values were observed in samples with the chemical composition $Cu_{40}Zr_{45}Al_5Ag_{10}$. Using the nanoindenter, the modulus of elasticity was determined through the Oliver-Pharr method, which analyzes the slope of the unloading curve of the indenter. Multiple measurements were conducted to ensure statistical reliability. No cracks appeared around the indentations, indicating the material's strength and uniformity under the applied load.

Tabel 4 Micro-Vickers and nanoindentation results

Chemical composition	Master alloys Micro-Vickers (HV)	Ribbons Micro-Vickers (HV)	Rods Micro-Vickers (HV)	Ribbons nanoindentation (HV)	Ribbon Young Modulus (GPa)
$Cu_{40}Zr_{45}Al_5Ag_{10}$	605.6		686	593.1185	95.27
$Cu_{45}Zr_{45}Al_5Ag_5$	519.2	577.6	644	570.1087	94.08791
$Cu_{50}Zr_{45}Al_5$	404	485.4	519.2	532.3969	92.91182

The sample $Cu_{40}Zr_{45}Al_5Ag_{10}$, with the highest hardness and modulus of elasticity, demonstrates superior resistance to deformation. The sample $Cu_{45}Zr_{45}Al_5Ag_5$ also shows strong mechanical performance, although slightly lower compared to the sample with 10% Ag composition. In contrast, the sample $Cu_{50}Zr_{45}Al_5$, shows the lowest hardness and modulus of elasticity.

Characterization of mechanical properties: Tensile tests

The tensile testing of ribbons faces significant challenges due to their shape and distinctive properties. A major issue was the clamping system used to secure the samples in the testing apparatus without inducing undesirable deformations. This aspect could compromise the accuracy of the measurements.

To address this challenge, the Department of Mechanics and Materials Resistance developed a customized clamping system. This innovative clamping solution ensured a secure and firm grip on the ribbons without causing damage, allowing for more accurate and reliable results in the tensile tests. The clamping solution for the ribbons is illustrated in figure 14.

Fig. 14: New method to hold ribbons

Another issue during the tensile testing was the surface and edges of the ribbons, which exhibited irregularities and small defects due to the manufacturing technology.

During the testing of the ribbons, it was observed that many samples failed in areas with edge irregularities or surface defects. The adopted solution was to coat the ribbons with a layer of epoxy resin (Epoxy BK) to smooth out the surface irregularities and fill any micro-pores. This approach improved the mechanical stability of the samples during testing. The three chemical compositions were tested for each sample, along with a reference sample of pure resin. The coating process involved pouring the resin over the ribbons, which were placed in a silicone mold (figure 15) to prevent resin leakage. After pouring the resin, the mold was carefully positioned in a vacuum chamber to prevent additional material defects. The next step was to extract the samples from the mold.

Tabel 5 R_m results of ribbons before and after applying epoxy resin coating

Sample	Ribbon R_m (MPa)	Epoxy resin coated ribbons R_m (MPa)
$Cu_{40}Zr_{45}Al_5Ag_{10}$	1029.26	1978.12
$Cu_{45}Zr_{45}Al_5Ag_5$	1009.17	1473.6

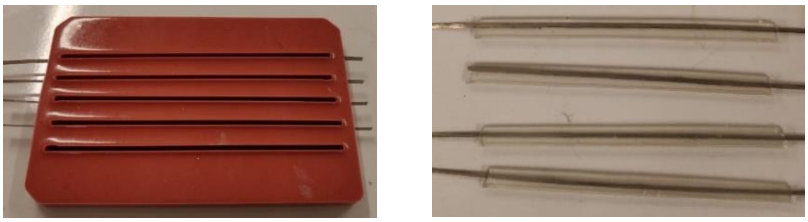

Fig. 15: Mold to apply coating and Ribbons covered with epoxy resin

The tensile results of the uncoated ribbons were compared with those of the ribbons coated with a resin layer. Figure 16 shows the tensile curves of the ribbons covered with epoxy resin. Improved values were observed for the modulus of elasticity: for the sample with 5% Ag (before the resin layer was applied), the modulus value was 30,872 MPa, while after applying the layer, it increased to 154,400 MPa. Better results were also noted for elongation: for the sample with 5% Ag (before the resin layer was applied), the elongation was 0.027%, and after applying the layer, it increased to 1.3%.

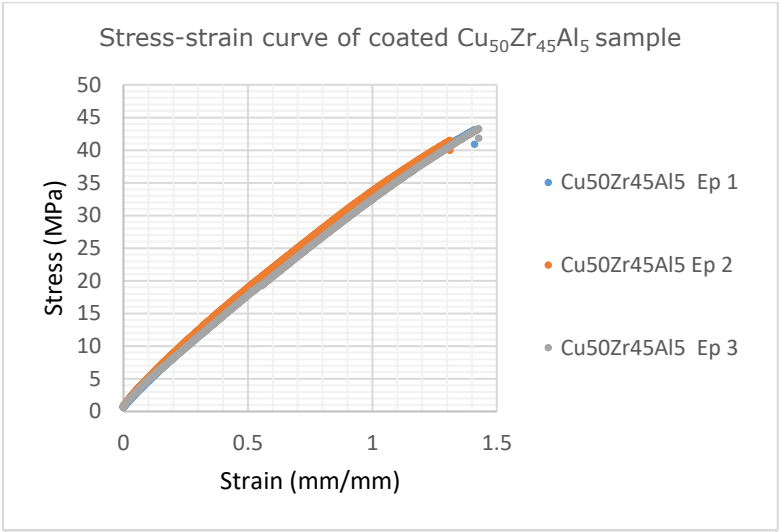

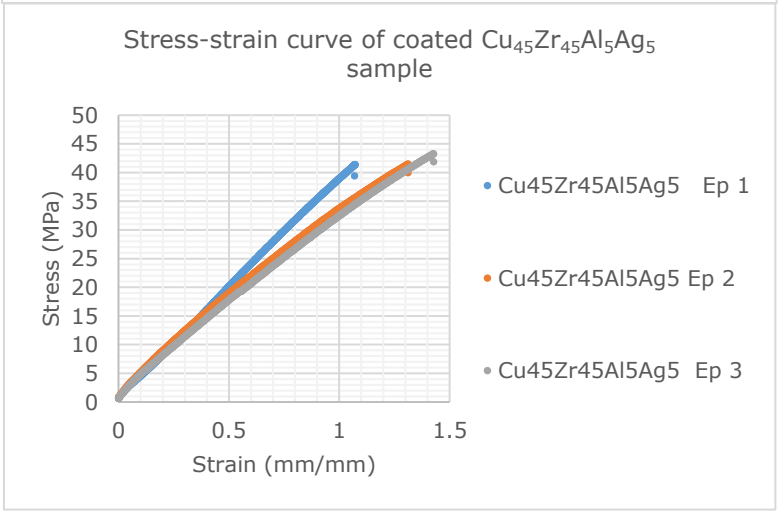

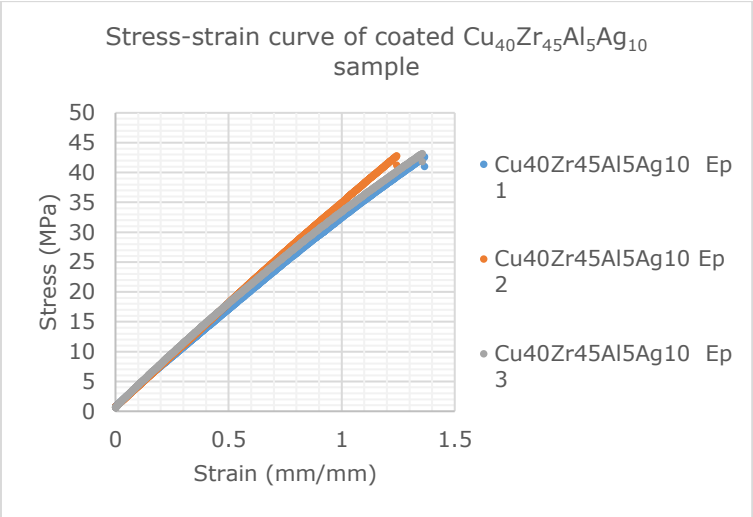

Fig. 16: Tensile curves of coated ribbons

By applying a method of estimation proposed by Jones [22]: the micromechanics equations method, the goal was to evaluate the modulus of elasticity and mechanical strength of the ribbons coated with a resin layer. This method takes into account the equal deformation of both the matrix and the ribbons and uses a formula that considers the contribution of each component based on its volume fraction. This approach allows for the isolation and more accurate assessment of the ribbons' strength, thereby reflecting their mechanical behavior strictly. The tensile strength value (R_m) for the sample with 10% Ag was obtained as 1978.12 MPa. We can conclude that this estimation method enables the determination of the mechanical properties of amorphous metal ribbons while eliminating the effect of the resin coating.

Analysis of the deformation behavior of amorphous ribbons

The next step was to determine and evaluate the deformation behavior of the ribbons when subjected to nanoindentation. The deformation behavior in the area of the Berkovich indenter was evaluated. By applying the calculation method based on the penetration depth it was possible to determine the effective depth remaining after the withdrawal of the indenter. Thise data, correlated with the hardness of the material, contribute to the calculation of a final ratio h_f/h_{max} which shows that the ribbons have a rigid-plastic behavior.

Tabel 6 Ratio of the residual depth h_f to the max depth h_{max}

Parameter	$Cu_{45}Zr_{45}Al_5Ag_5$	$Cu_{40}Zr_{45}Al_5Ag_{10}$	$Cu_{50}Zr_{45}Al_5$
h_f/h_{max} (nm)	0.776070848	0.784860419	0.791926277

While nanoindentation provides accurate localized measurements of hardness, it does not directly provide macroscopic mechanical properties. To overcome this, an analytical model is proposed to determine the yield strength of materials using data from nanoindentation and applying Tabor's relation [23]. Values close to those resulting from traction were determined. This is consistent with established findings that nanoindentation provides reliable measurements of elastic modulus and yield strength, particularly in materials such as amorphous alloys.

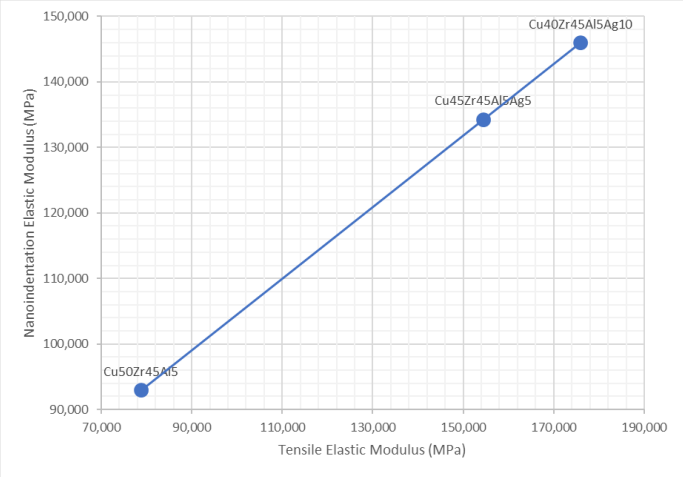

Fig. 17: Comparison of elastic modulus obtained from nanoindentation and tensile tests

The values of the elasticity modulus obtained by nanoindentation and tensile tests do not show significant differences (as can be seen in figure 17). The analytical model used in this study, based on the Tabor relation and adjusted for the actual contact area and indentation depth parameters, provides an effective prediction of yield strength and modulus of elasticity. It also provides a deeper insight into how compositional changes influence deformation mechanisms.

Characterization of chemical properties

For the evaluation of chemical properties, a procedure was employed to assess the ion leaching from the ribbons into a container with deionized water. The objective of this assessment is to measure the conductivity of the deionized water in which the ribbons were immersed. This conductivity measurement provides insights into the amount of ions released into the solution, which can reflect the chemical stability of the material.

The test was conducted over two time periods: 24 hours and 168 hours at 80°C. The samples were submerged in a borosilicate glass container with a polypropylene lid, which contained deionized water. Measurements were taken using a portable conductivity tester. As ions leach into the water, the conductivity increases, which may indicate material degradation. Conductivity was measured at both the beginning and the end of the test.

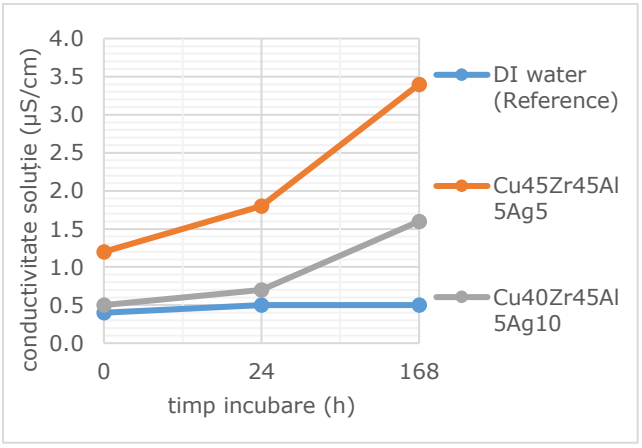

Fig. 18: Ion leaching method

The $Cu_{45}Zr_{45}Al_5Ag_5$ samples showed visible degradation after 24 hours, but after 168 hours, the sample almost disintegrated. The absence of visible defects in the $Cu_{40}Zr_{45}Al_5Ag_{10}$ sample can be attributed to the improved corrosion resistance and structural integrity of the alloy.

Chapter 5 Applications of amorphous based Cu-Zr-Al(-Ag) alloys

Applications in composites manufacturing

Studies have been carried out on composites having a matrix of acrylic resin and silicone, and the reinforcement was the amorphous ribbons.

A mold was made using 3D printing technology (according to the DIN ISO 527-4 standard) to hold the amorphous ribbons in a fixed position and over which the polymer matrix was poured. This allowed safe release from the mold and prevented chemical interaction between the mold and the resin.

Fig. 19: Tensile test of a composite reinforced with amorphous ribbons

Acrylic resin was selected due to its good properties: tensile strength and elastic modulus. To evaluate the effectiveness of this reinforcement, composites were reinforced with two or three bands (with the chemical composition $Cu_{45}Zr_{45}Al_5Ag_5$ and $Cu_{40}Zr_{45}Al_5Ag_{10}$). Additionally, a reference sample of unreinforced acrylic resin was produced. Positive results were obtained in comparison with the 2-ribbon reinforced composites. But on closer inspection, air bubbles were observed around the ribbon and in some cases due to lack of adhesion, the reinforcement slipped from the matrix at the time of tensile failure. Therefore, the composites were placed in a vacuum chamber to eliminate potential defects. Thus, the tensile curve (figure 20) was obtained for 3-ribbon reinforced composites. Better traction behavior compared to the reference is observed. This result confirms that the bands are reinforcing, providing higher values compared to the reference.

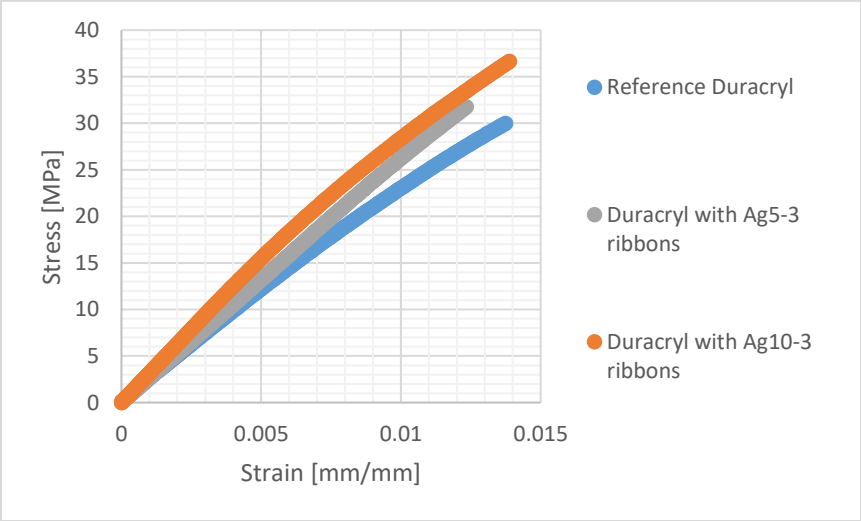

Fig. 20: Tensile curve for 3-ribbon reinforced composites

Tensile tests were also performed on composites having a silicone matrix. As a reinforcement, amorphous ribbons inserted in knitted form were used as can be seen in figure 21, but also simple ribbon arranged along the sample. The purpose of these tests was to determine whether the addition of ribbons, independent of their composition, could improve the mechanical properties of the composite.

Fig. 21: Knitted ribbons used as reinforcement in the silicone matrix

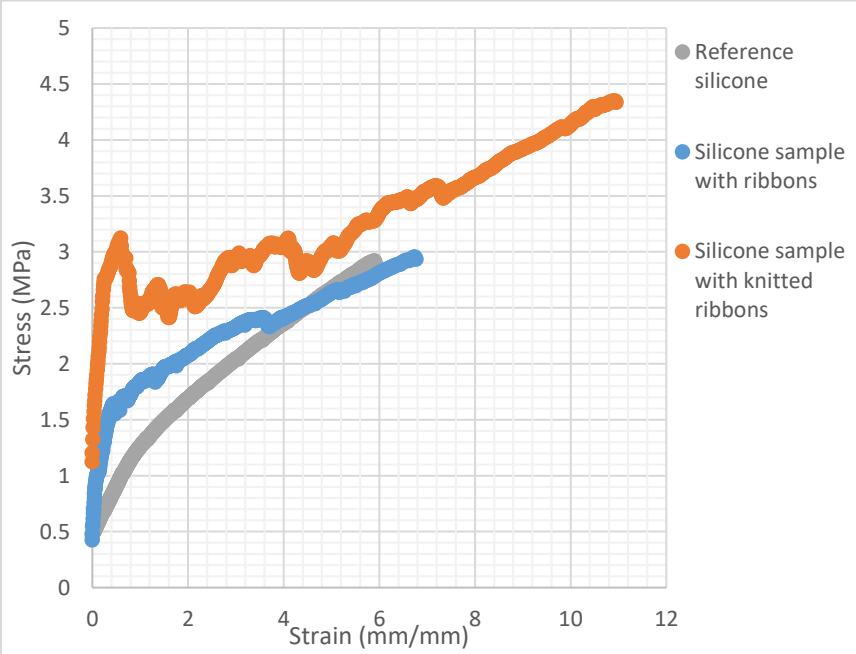

Fig. 22: Silicone matrix composite tensile curve

In the case of the composites with the acrylic resin polymer matrix, an increase in the elastic modulus was observed. The effect of 3-ribbon reinforcement and the improvement of the composites process in the vacuum chamber led to higher values of mechanical stress and relative elongation. Silicone matrix composites reinforced with braided ribbons show better mechanical fracture resistance (figure 22), indicating an improvement in mechanical properties.

Applications of welded ribbons or embedded in functional structures

Joining of amorphous ribbons by welding

To unlock the full potential of amorphous materials in engineering applications, the need for innovative joining technologies has become increasingly evident. That is why in this subchapter a comparative study of the different methods of welding the ribbons has been carried out to see which method offers the best results in terms of preserving the amorphous structure.

The welding techniques on which the experimental studies were carried out were :

- Electron beam welding (EBW)
- Electric Resistance Spot Brazing (ERSB)
- Resistance spot welding (RSW)
- Ultrasonic Welding (UW)
- Spot welding (SW)

Ultrasonic welding and spot-welding equipment were provided by the National Institute for Research and Development in Welding and Materials Testing (ISIM), and Materials and Manufacturing Engineering.

Ultrasonic welding has shown promising results to join amorphous metal alloys. Several attempts were made to reach the optimal parameters that gave satisfactory results (sonotrode pressure on the samples, welding time). With the help of the electron microscope, the successful joining of the ribbons was confirmed (figure 23), and X-ray diffractometry shows that the amorphous structure was preserved in the weld area (figure 24).

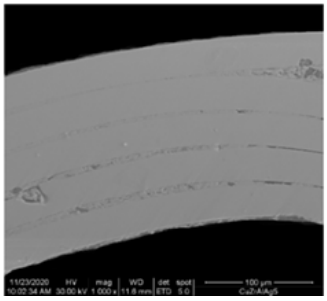

Fig. 23: Ultrasonic welding on ribbons

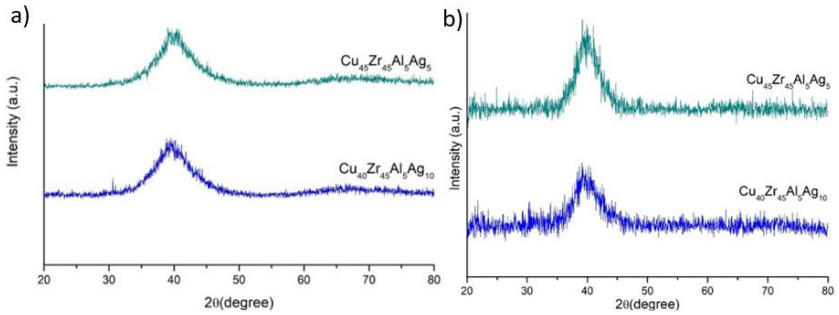

Fig. 24: XRD results: before welding (left), after welding (right)

The investigation of the surfaces of the ribbons subjected to spot welding, using the scanning electron microscope, shows that they have been welded (figure 25) and X-ray diffractometry in the weld area shows that the amorphous structure has been preserved (figure 26).

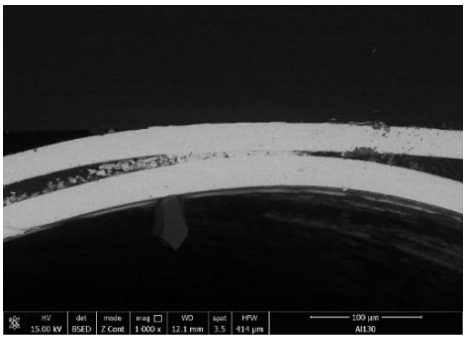

Fig. 25: Welded area of ribbons by spot welding

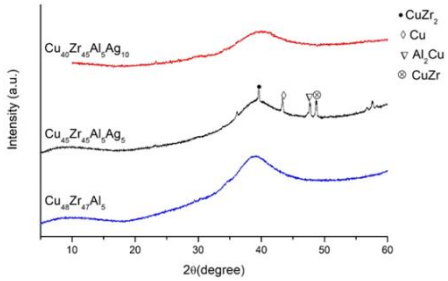

Fig. 26: XRD analysis on the weld area

Ultrasonic welding did not structurally affect the ribbons, and differential calorimetry corresponds to an amorphous structural state. Spot welding is a promising method for joining the ribbons: EDX confirms the preservation of the chemical composition and XRD shows the preservation of the amorphous structure. Electron microscopy offers the best method of evaluating the joint area, since at a macroscopic level they can give the impression of a successful joint. Both the UW and RSW methods had minimal thermal impact on the ribbons as indicated by the DSC temperature profiles.

Applications of amorphous Cu-Zr-Al-Ag metallic ribbons as nanoporous structures

During this subchapter the use of amorphous metal ribbons in applications as nanoporous structures has been pursued. Obtaining nanoporous layers can be done through several processes. In the present case, the ribbons were subjected to the dealloying process. By dealing in hydrofluoric acid (HF), certain elements of the chemical composition dissolve, and this leads to the creation of nanoporous structures. In practical terms, nanoporous ribbons synthesized by dealloying can exhibit a wide spectrum of properties that make them applicable in range of applications. One such application refers to the study of the adhesion of water droplets to the surface of the ribbons.

The ribbons were soaked in HF of different molar concentrations: 0.5M, 0.4M, 0.3M, 0.2M, 0.1M, 0.05M and 0.01M and the immersion time varied between 2, 5, 10 and 20 minutes, with one end fixed to a support. SEM images and EDX analysis demonstrate the selective dissolution of alloying elements, especially Al and Zr, leading to pore formation.

The application aimed to demonstrate that this nanoporous structure supports a drop of water deposited on the lower surface of the ribbon against the force of gravity.

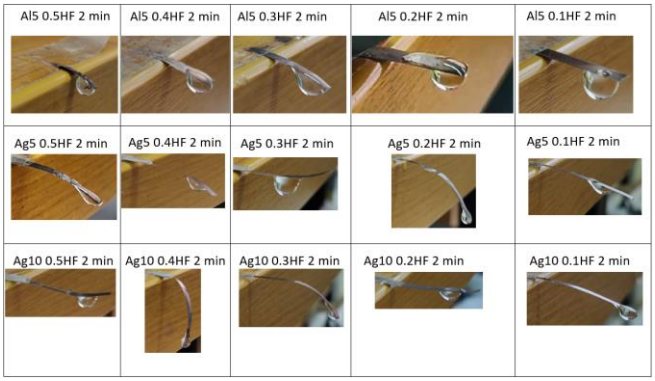

Fig. 27: Example of a drop applied to ribbons

The droplet was monitored to see where on the ribbons' surface it adhered, how long it adhered, and whether after applying small shocks, it still adhered on it. Water adhesion evaluation testing shows that an increase in HF concentration and duration leads to increased droplet adhesion and ribbon bending. By optimizing the dealloying conditions, nanoporous structures could be used in various industries for the purpose of surface protection, self-cleaning and adhesion improvement.

Also in this subchapter, it was investigated whether the dealloyed ribbons in HF offer a possible solution for separating water from an oil-water mixture. Two types of oils were used: domestic and automotive, and 0.5M HF dealloyed ribbon were used. Since the dealloyed ribbons in HF creates a porous structure, they were used as a filtering method for the two mediums. UV-VIS spectroscopy was used to evaluate the filtration efficiency. The absorption spectrum of the filtered water was measured; this was compared to the spectrum of a reference sample (water that did not go through the filtration process).

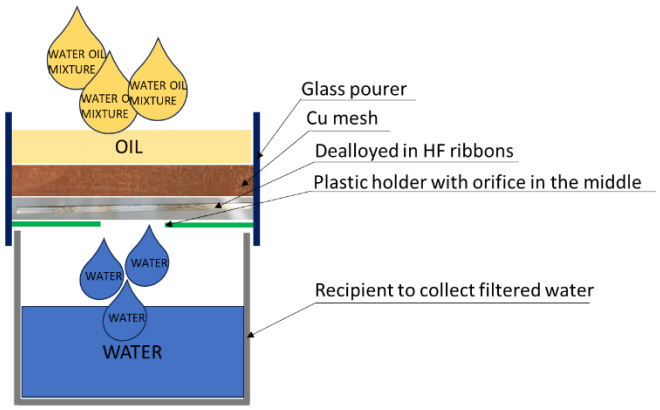

Fig. 28: Schematic representation of filtering method

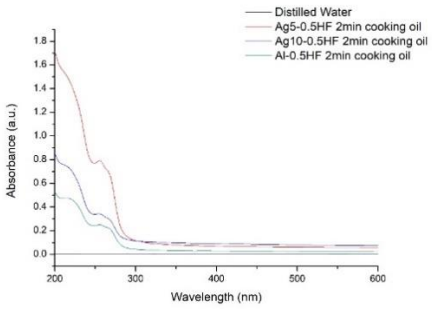

Fig. 29: UV-VIS spectra of 0.5HF dealloyed ribbons for 2 min filtering automotive oil

It was shown that the Cu-Zr-Al-Ag alloy with 10% Ag consistently showed the lowest absorption peaks (according to UV-VIS investigations), indicating superior filtration performance especially for automotive oils.

Chapter 6 Conclusions, future directions

Conclusions

In this last chapter, general conclusions, personal contributions and possible future directions are presented.

The research within this thesis had as the starting point obtaining metallic alloys with an amorphous structure from elements of medium technical purity, in an uncontrolled atmosphere, in the form of ribbon and rods, then aiming at their structural characterization, the determination of the mechanical, chemical and some possible applications.

Based on the obtained results, the following conclusions can be reached:

- The cooling rate, roll speed and melt ejection pressure during the ribbon making process, along with the chemical composition, have a direct impact on the structure and quality
- Additional alloying with Ag (with 10%) of alloys based on Cu-Zr-Al whose components chemical elements have an average technical purity is a necessary condition for favoring the obtaining of amorphous structure
- XRD analysis confirmed the amorphous nature of the ribbons and rods for the alloy $Cu_{40}Zr_{45}Al_5Ag_{10}$
- Tensile test results of the ribbons were influenced by surface irregularities, which acted as crack initiation sites, leading to low mechanical tensile strength
- The solution adopted to cover the ribbons with a very thin layer of epoxy resin (Epoxy BK) led to the "elimination" of the existing stress concentrator and a more even distribution of stresses. Applying the micro-mechanics equations and the Kelly-Davies relations to determine R_m in the case of composites (in the present case the ribbon is the reinforcement, the coating being the matrix) resulted in high values of the breaking strength similar to those existing in the specialized literature.
- The alloy $Cu_{40}Zr_{45}Al_5Ag_{10}$ exhibited superior corrosion resistance
- The incorporation of ribbons into the acrylic resin matrix improves the stiffness and mechanical strength of the resulting composite, provided that the ribbons are carefully prepared to avoid a decrease in ribbon-matrix adhesion and that there is a minimum fiber volume of at least 2% of metallic glass
- Spot welding (UW and RSW methods) proved to be an effective method of joining Cu-Zr-based ribbons, offering strong joints, without significant thermal damage in the joint area, thus preserving the amorphous structure of the ribbons
- Cu-Zr-Al-Ag amorphous alloys can form nanoporous structures through dealloying processes in HF with adhesion-related applicability. Wetting tests show that both higher HF concentrations and immersion durations lead to increased water droplet adhesion and ribbon bending. This suggests that surface modification has an impact on the wettability and functional properties of the ribbons with applications in surface protection, self-cleaning
- Another application of the ribbons as nanoporous structures developed in the thesis concerns their filtering capacity. The differences in filtration performance between ribbons for the three types of Cu-Zr-Al-Ag based alloys highlight the impact of alloy composition on filtration efficiency and affect the material's ability to filter

different types of oils from water. Ribbons containing 10% silver demonstrated the best oil filtration efficiency as demonstrated by UV-Vis spectroscopy

Personal contributions are:

- Obtaining metal alloys with an amorphous structure based on Cu-Zr-Al in the form of ribbons and rods, using chemical elements of medium purity as raw materials, by additional alloying with 10% Ag
- Structural characterization, from a mechanical (traction, hardness) and chemical (corrosion tests) point of view, of the ribbons and rods obtained; the obtained properties are close to metallic glasses based on Cu-Zr or Cu-Zr-Al obtained from high purity chemical elements
- Promote as an innovative procedure for fixing the ribbons and eliminating the crack initiation effect due to edge irregularities in the tensile test, which led to a significant reduction in measurement errors
- The implementation with remarkable results of the joints of amorphous metal ribbons by spot welding
- Processing amorphous metal ribbons based on Cu-Zr-Al-Ag by dealloying as nanoporous structures for innovative applications: water adhesion to the surface of the ribbons, filtration of oil-water mixtures

Future directions

The theoretical and experimental studies carried out opened new directions for future research, among which are considered more relevant:

- Obtaining new families of amorphous alloys using medium purity chemical elements as raw materials by identifying new alloying elements or combinations that improve the glass-forming ability, thermal stability and chemical and physical mechanical properties of the alloys
- Exploring the integration of amorphous metal alloys in various forms (in low percentages) in the development of hybrid composites with polymer or ceramic matrices for specific applications.
- Development of new applications for amorphous ribbons and rods in fields such as catalysis of hydrogenation, oxidation processes, etc., as nanoporous structures with fine, controlled porosity created through dealloying

Selective bibliography:

1. Li, L., et al., *Recent Advances of Amorphous Nanomaterials: Synthesis and Applications.* Chinese Journal of Chemistry. **n/a**(n/a).
2. Guo, T., et al., *Amorphous materials emerging as prospective electrodes for electrochemical energy storage and conversion.* Chem, 2023. **9**(5): p. 1080-1093.
3. Cao, X. and M. Sun, *Molecular dynamics simulation of minor Zr addition on short and medium-range orders of Cu-Zr metallic glass.* J Mol Model, 2022. **28**(10): p. 324.
4. Kbirou, M., et al., *Structural Correlation of the Glass-Forming Ability in a Cu–Zr-Based Metallic Glass: A Molecular Dynamics Study.* physica status solidi (b), 2024. **261**(8): p. 2400100.
5. Prabhu, Y., et al., *Crystallization kinetics and nanoindentation studies of Cu46Zr40Ti8.5Al5.5 glassy alloy.* Journal of Non-Crystalline Solids, 2024. **625**: p. 122753.
6. Wang, Q., et al., *Composition optimization of the Cu-based Cu–Zr–Al alloys.* Intermetallics,

2004. **12**(10-11): p. 1229-1232.
7. Jiang, S.-S., et al., *A CuZr-based bulk metallic glass composite with excellent mechanical properties by optimizing microstructure.* Journal of Non-Crystalline Solids, 2018. **483**: p. 94-98.
8. Gammer, C., et al., *Influence of the Ag concentration on the medium-range order in a CuZrAlAg bulk metallic glass.* Sci Rep, 2017. **7**: p. 44903.
9. Li, B., et al., *Effects of Ag substitution for Fe on glass-forming ability, crystallization kinetics, and mechanical properties of Ni-free Zr–Cu–Al–Fe bulk metallic glasses.* Journal of Alloys and Compounds, 2020. **827**: p. 154385.
10. Bokas, G.B., et al., *Microalloying effects in ternary Cu-Zr-X (X = Be, Mg, Al, Si, P, Nb, Ag) icosahedral clusters and super-clusters from Density Functional Theory computations.* Polyhedron, 2017. **133**: p. 1-7.
11. Louzguine-Luzgin, D.V., et al., *Glass-forming ability and differences in the crystallization behavior of ribbons and rods of Cu36Zr48Al8Ag8 bulk glass-forming alloy.* Journal of Materials Research, 2011. **24**(5): p. 1886-1895.
12. Dan, Z., et al., *Fabrication of nanoporous copper by dealloying of amorphous Ti–Cu–Ag alloys.* Journal of Alloys and Compounds, 2014. **586**: p. S134-S138.
13. Zhou, Y., et al., *Fabrication of Superhydrophobic Porous Brass by Chemical Dealloying for Efficient Emulsion Separation.* Molecules, 2023. **28**(18): p. 6509.
14. Zhang, T., K. Kurosaka, and A. Inoue, *Thermal and Mechanical Properties of Cu-Based Cu-Zr-Ti Bulk Glassy Alloys.* Materials Transactions - MATER TRANS, 2001. **42**: p. 2042-2045.
15. Inoue, A. and W. Zhang, *Formation, thermal stability and mechanical properties of Cu-Zr-Al bulk glassy alloys.* Materials Transactions, 2002. **43**(11): p. 2921-2925.
16. Greer, A.L. and E. Ma, *Bulk Metallic Glasses: At the Cutting Edge of Metals Research.* MRS Bulletin, 2011. **32**(8): p. 611-619.
17. Angell, C.A., *Spectroscopy simulation and scattering, and the medium range order problem in glass.* Journal of Non-Crystalline Solids, 1985. **73**(1): p. 1-17.
18. Wang, W.-H., et al., *Elastic constants and their pressure dependence of Zr41Ti14Cu12.5Ni9Be22.5C1 bulk metallic glass.* Applied Physics Letters, 1999. **74**(13): p. 1803-1805.
19. Chen, H.S., *Glassy metals.* Reports on Progress in Physics, 1980. **43**(4): p. 353.
20. Kaban, I., et al., *Atomic structure and formation of CuZrAl bulk metallic glasses and composites.* Acta Materialia, 2015. **100**: p. 369-376.
21. Cosmin Codrean, V.-A.S., *Metale amorfe si Nanocristaline*. 2007: Editura Politehnica.
22. Jones, R.M., *Mechanics Of Composite Materials*. 2nd Edition ed, ed. C. Press. 2018: Boca Raton.
23. Zhang, P., S.X. Li, and Z.F. Zhang, *General relationship between strength and hardness.* Materials Science and Engineering: A, 2011. **529**: p. 62-73.